

## Viruses as mortality agents of picophytoplankton in the deep chlorophyll maximum layer during IRONAGES III

Anne-Claire Baudoux, Marcel J. W. Veldhuis, Harry J. Witte, and Corina P. D. Brussaard<sup>1</sup>

Department of Biological Oceanography, Royal Netherlands Institute for Sea Research, P.O. Box 59, NL-1790 AB Den Burg, The Netherlands

### Abstract

We report viral-induced mortality rates of the picoeukaryotic (two size classes) and prokaryotic (cyanobacteria *Prochlorococcus* and *Synechococcus*) phytoplankton during a cruise in the oligotrophic subtropical northeastern Atlantic (October 2002). A dilution assay, simultaneously estimating viral lysis and microzooplankton grazing, was applied around the deep chlorophyll maximum (DCM) at six stations. For the smallest picoeukaryotes (group I), viral lysis was responsible for 50–100% of the total cell losses, with rates ranging from 0.1 to 0.8 d<sup>-1</sup>. Viral lysis rates were positively linked to the abundance and contribution of large genome-sized (180–225 kb) putative algal viruses. In contrast, the prokaryotic picophytoplankton did not seem to be controlled by viral lysis. For *Synechococcus*, microzooplankton grazing dominated, with rates between 0.1 and 0.25 d<sup>-1</sup> (comparable to those for the eukaryotic algae). For *Prochlorococcus*, both viral lysis and microzooplankton grazing rates were very low (0–0.1 d<sup>-1</sup>). Overall, the total carbon production by the picophytoplankton community was balanced by the combined losses due to viral lysis and microzooplankton grazing. Viral lysis released 0.1–0.3 μg of picophytoplanktonic C L<sup>-1</sup> d<sup>-1</sup>, which comprised 21% of the total carbon production by picophytoplankton.

Phytoplankton communities in oligotrophic open oceans are usually dominated by picophytoplanktonic cells (<3 μm), including eukaryotes and prokaryotes (Partensky et al. 1996). The prokaryotic component is represented by the cyanobacteria *Synechococcus* and *Prochlorococcus* (Partensky et al. 1996). The picoeukaryotes are less investigated than the prokaryotes, but their contribution to the total carbon biomass and the ecosystem productivity can be substantial (Li 1994; Partensky et al. 1996; Worden et al. 2004). Recent publications describe dynamics in abundance (Worden et al. 2004) and a high degree of species diversity within this group (Moon-van der Staay et al. 2001; Veldhuis and Kraay 2004).

Picophytoplanktonic cells possess a high growth rate, despite the very low concentrations of macronutrients characterizing oligotrophic habitats (Partensky et al. 1996; Worden et al. 2004). Their ecological success in oligotrophic waters has mainly been attributed to their small size because the relatively high surface area to volume allows maximal uptake to sustain the cell metabolism (Raven 1998). Among the loss factors regulating picophytoplankton populations, grazing is considered important (Quevedo and Anadón 2001; Worden et al. 2004), whereas sedimen-

tation is thought to be negligible, considering their micrometer size range (Raven 1998). Besides grazing, there are indications that cell lysis contributes to phytoplankton loss in oligotrophic systems (Agusti et al. 1998). One of the factors causing cell lysis is viral infection, and currently, host-specific viruses are reported for photosynthetic prokaryotes (for a review, see Mann 2003) as well as picoeukaryotes (for a review, see Brussaard 2004a). Phytoplankton losses caused by cell lysis and grazing influence the flow of nutrient and energy in different ways. The release of cell constituents upon lysis directly affects the standing stock of dissolved organic carbon and the recycling of nutrients, whereas grazing channels phytoplankton biomass to the higher trophic levels (Wilhelm and Suttle 1999). Therefore, the relative effects of viruses and microzooplankton need to be assessed for optimally understanding biogeochemical cycling.

Studies that encompass oligotrophic sites show high numerical abundance and a diverse and dynamic virus community for both cyanophages and algal viruses (Short and Suttle 2003; Mühling et al. 2005). This implies that viruses are responsible for algal mortality. Actual viral lysis rates of photosynthetic organisms in oligotrophic systems are, however, poorly documented. The few existing studies suggest that between 0.6% and 8% d<sup>-1</sup> of the standing stock of *Synechococcus* undergoes viral lysis in oligotrophic waters (Waterbury and Valois 1993; Garza and Suttle 1998). These values were, however, obtained by theoretical conversion factors and calculations. A specific assay that allows a direct estimation of viral-induced algal mortality has been developed recently (Evans et al. 2003). This viral dilution assay has been successfully applied for the picophytoplankton *Micromonas pusilla* (Evans et al. 2003) during a mesocosm study and the nanophytoplankton *Phaeocystis globosa* during a field study in temperate eutrophic coastal waters (Baudoux et al. 2006). The viral

<sup>1</sup> Corresponding author (corina.brussaard@nioz.nl).

### Acknowledgments

We thank the captain and crew of the RV *Pelagia*. We thank especially chief scientist Klaas Timmermans for the opportunity to join the IRONAGES III cruise. We thank Marieke Bossink, Margriet Hiehle, Nelleke Krijgsman, Swier Oosterhuis, and the nutrient service laboratory for technical support. The reviewers as well as the associate editor are acknowledged for their constructive comments on the manuscript. This study was supported by the Research Council for Earth and Life Sciences (ALW) with financial aid from the Netherlands Organization for Scientific Research (NWO).

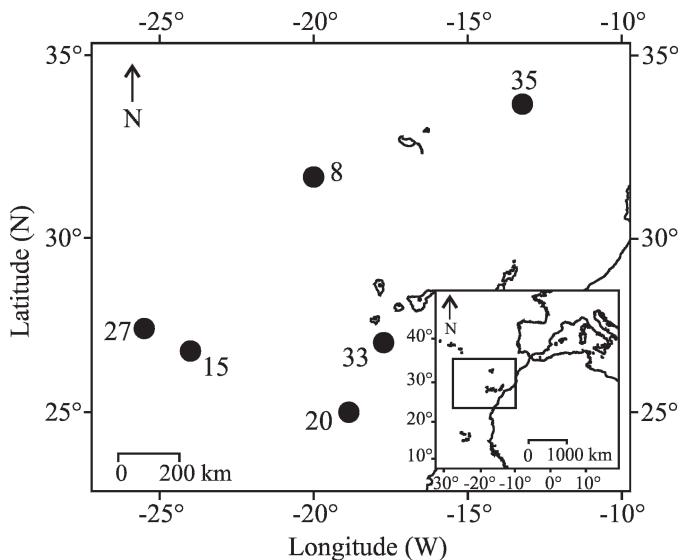


Fig. 1. Location of the sampling stations during the IRON-AGES III cruise (Ponta Delgada, Azores, Portugal—Valencia, Spain; 03–29 October 2002).

lysis dilution assay has, as yet, never been applied in an oligotrophic ecosystem. During this study, we used the viral lysis dilution assay to elucidate the relevance of virus-induced mortality in picophytoplankton of the oligotrophic subtropical northeastern Atlantic. Viral lysis rates were determined across the different groups (prokaryotes as well as eukaryotes) forming the picophytoplankton community and compared with microzooplankton grazing.

## Materials and methods

**Study area and sampling**—Six stations were investigated aboard the RV *Pelagia* from 03 to 29 October 2002 during the IRONAGES III shipboard expedition (Fig. 1; Table 1). Samples were collected with 10-liter NOEX bottles mounted on the Rosette sampler equipped with a Seabird conductivity–temperature–depth (CTD) sensor and a photosynthetically active radiation (PAR) detector. The sampling was

performed around the deep chlorophyll maximum (DCM) according to the highest in vivo fluorescence as detected by a fluorometer set up on the CTD rosette (Table 1).

Discrete samples for nutrients (5 mL) were filtered through 0.2- $\mu\text{m}$ -pore-size polysulfone filters (Acrodisc, Gelman Sciences). Analyses were performed on board with a TrAAcs 800 autoanalyzer for dissolved inorganic nutrients (N, P, and Si) as described in Baudoux et al. (2006). Chlorophyll *a* (Chl *a*) samples of typically 1.5 liters were filtered onto a GF/F filter (Whatman) and stored at  $-80^{\circ}\text{C}$  until analysis. Chl *a* was extracted in 90% acetone and measured fluorimetrically.

**Phytoplankton**—Phytoplankton abundance from natural as well as experimental samples was enumerated directly after sampling with a modified Beckman Coulter XL-MCL flow cytometer. To increase the instrument sensitivity, the flow rate of the sheath fluid was reduced, and the band-pass filter in the red detector was removed to increase the spectral fluorescence band. The instrument was equipped with a laser with an excitation wavelength of 488 nm (15 mW) and emission bands for the chlorophyll autofluorescence ( $>630$  nm) and phycoerythrin ( $575 \pm 20$  nm). The discriminator for phytoplankton was the red chlorophyll autofluorescence. Flow rate ( $135 \pm 7 \mu\text{L min}^{-1}$ ) and machine drift were checked every day with calibrated beads (Flow-Check Fluorospheres, Beckman Coulter) as the internal standard. A maximal volume of 1.5 mL per sample was analyzed. Based on the pigment autofluorescence and forward scatter, we discriminated the prokaryotes *Prochlorococcus* spp. and *Synechococcus* spp., as well as two populations of picoeukaryotes (Fig. 2A). *Synechococcus* spp. were discriminated from the other phytoplankton on the basis of the presence of their orange autofluorescence caused by the accessory pigment phycoerythrin. The division of the picoeukaryotes was based on their relative size by the approach of Veldhuis and Kraay (2004); the picoeukaryote group I had a cell diameter ranging from 1.3 to 1.5  $\mu\text{m}$ , and group II ranged from 1.5 to 2.5  $\mu\text{m}$ .

Phytoplankton carbon biomass was derived from cellular carbon content of the specific phytoplankton. We used an

Table 1. Location and characteristics of the studied stations.

	Station					
	8	15	20	27	33	35
Latitude (N)	31.71	26.78	25.00	27.43	27.03	33.70
Longitude (W)	20.00	24.00	18.86	25.50	17.73	13.22
Depth sample (m)	100	100	70	70	60	80
Temperature ( $^{\circ}\text{C}$ )	18.2	20.1	19.6	23.0	23.0	17.7
Salinity	36.59	36.86	36.42	37.09	36.75	36.39
$\text{NO}_3$ ( $\mu\text{mol L}^{-1}$ )	0.05*	0.06*	1.52	0.02*	0.03*	0.01*
$\text{NO}_2$ ( $\mu\text{mol L}^{-1}$ )	0.02	0.01	0.19	0.01	0.03	0.01
$\text{NH}_4$ ( $\mu\text{mol L}^{-1}$ )	0.10	0.13	0.33	0.02*	0.14	0.09
$\text{PO}_4$ ( $\mu\text{mol L}^{-1}$ )	0.02	0.02	0.17	0.02	0.02	0.01
Si ( $\mu\text{mol L}^{-1}$ )	0.61	0.54	0.55	0.41	0.42	0.49
Chl <i>a</i> ( $\mu\text{g L}^{-1}$ )	0.06	0.24	0.43	0.17	0.27	0.18

\* Value below the detection limit;  $0.008 \mu\text{mol L}^{-1}$  for  $\text{PO}_4$ ,  $0.08 \mu\text{mol L}^{-1}$  for  $\text{NO}_3$ ,  $0.008 \mu\text{mol L}^{-1}$  for  $\text{NO}_2$ ,  $0.03 \mu\text{mol L}^{-1}$  for  $\text{NH}_4$ , and  $0.1 \mu\text{mol L}^{-1}$  for Si. Standard deviations between runs were  $0.004 \mu\text{mol L}^{-1}$  for  $\text{PO}_4$ ,  $0.05 \mu\text{mol L}^{-1}$  for  $\text{NO}_3$ ,  $0.006 \mu\text{mol L}^{-1}$  for  $\text{NO}_2$ ,  $0.04 \mu\text{mol L}^{-1}$  for  $\text{NH}_4$ , and  $0.07 \mu\text{mol L}^{-1}$  for Si.

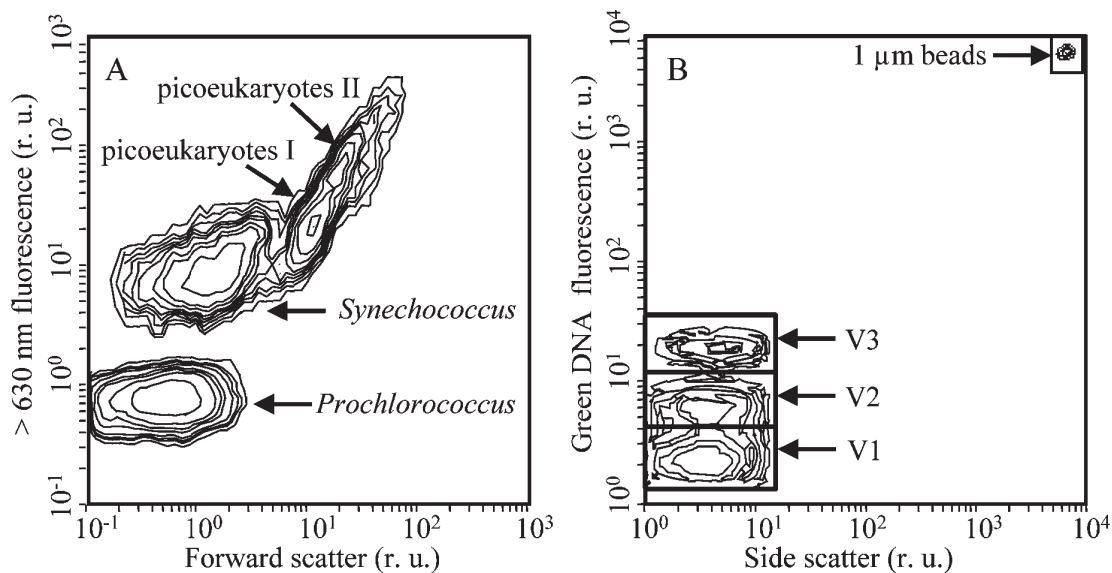


Fig. 2. Flow cytometric contour plots of (A) the typical phytoplankton community and (B) the typical virus community for the stations studied. The phytoplankton community is composed of the cyanobacteria *Prochlorococcus* and *Synechococcus* as well as two picoeukaryotic populations, with group I relatively smaller (1.3–1.5  $\mu\text{m}$ ) than group II (1.5–2.5  $\mu\text{m}$ ). The virus community is composed of three viral groups (V1, V2, and V3) discriminated on the basis of the intensity of their green fluorescence after staining with the nucleic acid-specific dye SYBR Green I. An internal standard (yellow-green fluorescent 1- $\mu\text{m}$  beads) was added to the sample.

averaged cellular carbon content of 46 fg C cell<sup>-1</sup> for *Prochlorococcus* (Bertlissou et al. 2003). For *Synechococcus* and the picoeukaryotes, the cellular carbon content was based on the cell biovolume, estimated by the calibration method of Veldhuis and Kraay (2004). Assuming phytoplankton cells to be spherical, we used a biovolume to carbon conversion factor of 254 fg C  $\mu\text{m}^{-3}$  for *Synechococcus*, derived from a carbon content of 213 fg C cell<sup>-1</sup> (Bertlissou et al. 2003). For the picoeukaryotes, we used a biovolume to carbon conversion factor of 239 fg C  $\mu\text{m}^{-3}$ , an average of the values obtained for *Ostreococcus* sp. CCE9901 (233–247 fg C  $\mu\text{m}^{-3}$ ; Worden et al. 2004) and *M. pusilla* CCMP 489 (238 fg C  $\mu\text{m}^{-3}$ ; DuRand et al. 2002).

*Viral lysis and microzooplankton grazing*—The viral-induced algal mortality as well as the microzooplankton grazing on phytoplankton were assessed simultaneously by an adapted version of the traditional dilution technique (Evans et al. 2003) with some modifications (Baudoux et al. 2006). A limitation of the dilution method is that the initial cell density must be sufficiently high to allow a three- to fourfold dilution with enough remaining cells present for accurate counting. During the present cruise, cell densities in surface waters were extremely low and did not meet this criterion. In contrast, numbers at the DCM were sufficiently high; therefore, the present study was restricted to the deeper waters.

The traditional dilution series of natural seawater with a 0.2- $\mu\text{m}$  filtered natural sample, which provided microzooplankton grazing rates (Landry and Hassett 1982), was combined with a second dilution series with a 30-kDa filtered natural sample, which provided the loss rates due to both grazing and viral lysis. Viral lysis rates were estimated from the difference between the two dilution series. All

material used for the experiments was carefully cleaned with 1 mol L<sup>-1</sup> HCl then, it was rinsed with MilliQ and finally with the same water from which the sample was collected. The experimental setup was conducted in a controlled room adjusted at in situ temperature (17–23°C) and under dimmed light. Around 08:00 h (local time), two 20-liter samples were carefully siphoned from the NOEX bottles into two 20-liter carboys, which were darkened to prevent light stress when the sample was brought on deck. The first 20-liter sample was filtered through a 0.2- $\mu\text{m}$ -pore-size polycarbonate filter (47 mm, Poretics, Millipore). A 5-liter aliquot was used as the 0.2- $\mu\text{m}$  diluent; the remaining sample was ultrafiltered through a 30-kDa polyether sulfone membrane filter (Pellicon filtration system, Millipore). The 30-kDa filtrate was used for generating the 30-kDa dilution series. The second 20-liter sample was presieved through 200- $\mu\text{m}$  mesh to remove larger zooplankton, and it was immediately used to set up the dilution series (20%, 40%, 70%, and 100% of natural water) with the 0.2- $\mu\text{m}$  and the 30-kDa diluent (3  $\times$  300 mL of soft polycarbonate incubation bottles). A 5-mL subsample was taken ( $T = 0$ ) upon filling. The incubation bottles were squeezed and closed in such a way that no air bubble was trapped in the bottle. All bottles were mounted on a slowly rotating (0.5 rpm) plankton wheel and incubated at temperature (17–23°C) and light intensity (10–37  $\mu\text{mol quanta m}^{-2} \text{ s}^{-1}$ , light period of 12 h) adjusted to in situ conditions given by the CTD and PAR detectors. After a 24-h incubation, another 5-mL subsample was taken to monitor phytoplankton growth. The apparent growth rate ( $\mu_{\text{app}}$ , d<sup>-1</sup>) was calculated for each sample from the changes in abundance during the incubation.

The regression coefficient of apparent growth rate versus dilution factor for the 30-kDa series represents the

phytoplankton losses due to microzooplankton grazing and viral lysis ( $M_{g+v}$ ,  $d^{-1}$ ), whereas the regression coefficient resulting from the 0.2- $\mu\text{m}$  dilution series represents only the microzooplankton grazing rate ( $M_g$ ,  $d^{-1}$ ). Specific viral-induced mortality rates ( $M_v$ ,  $d^{-1}$ ) were thus obtained from the difference between  $M_{g+v}$  and  $M_g$ . Specific growth rates ( $\mu$ ,  $d^{-1}$ ) were determined as the y-axis intercept value of the regression line obtained with the 30-kDa series. The significance ( $p$ ) of the slope ( $M_g$  and  $M_{g+v}$ ) and the intercept ( $\mu$ ) was determined by performing a  $t$ -test on the regression analysis. The significance ( $p$ ) between the slopes of the regression lines (i.e., significance of  $M_v$ ) was also estimated by a  $t$ -test.

A carbon budget was determined combining the cellular carbon content estimates (above section) and data of the dilution experiments. For each specific phytoplankton group, the carbon production (CP, in  $\mu\text{g C L}^{-1} \text{d}^{-1}$ ), carbon losses due to grazing ( $G$ , in  $\mu\text{g C L}^{-1} \text{d}^{-1}$ ), and, by adaptation, carbon losses due to viruses ( $V$ , in  $\mu\text{g C L}^{-1} \text{d}^{-1}$ ) were calculated by the formulas of Landry et al. (2000);  $CP = \mu \times P_m$ ;  $G = M_g \times P_m$ ;  $V = M_v \times P_m$ ; and  $P_m = P_0 \times [e^{(\mu - M_{g+v})t} - 1] / (\mu - M_{g+v})t$ , where  $\mu$  (in  $d^{-1}$ ) is the dilution-based specific growth rate (y-intercept of the 30-kDa regression),  $M_g$  and  $M_v$  (in  $d^{-1}$ ) are the dilution-based grazing and viral lysis rates,  $P_0$  (in  $\mu\text{g C L}^{-1}$ ) is the initial carbon biomass of picophytoplankton,  $P_m$  (in  $\mu\text{g C L}^{-1}$ ) is the geometric mean carbon biomass of picophytoplankton during the incubation, and  $t$  (in d) is the time of incubation.

**Virus abundance**—The abundance of viruses was determined on glutaraldehyde-fixed samples (final concentration, 0.5% glutaraldehyde, frozen in liquid nitrogen and stored at  $-80^\circ\text{C}$  prior to analysis) with a Becton-Dickinson FACSCalibur flow cytometer, with 15 mW of 488-nm air-cooled argon-ion laser according to Brussaard (2004b). Thawed samples were diluted (dilution factor  $>50$ ) in 0.2- $\mu\text{m}$  filtered autoclaved Tris-ethylenediamine-tetraacetic acid (EDTA) (TE) buffer (pH 8) and heated at  $80^\circ\text{C}$  for 10 min with the nucleic acid-specific dye SYBR Green I at a final concentration of  $5 \times 10^{-5}$  of the commercial stock (Molecular Probes, Invitrogen). Virus counts were corrected for the blank consisting of TE buffer with autoclaved 0.2- $\mu\text{m}$  filtered seawater in the correct dilution. An internal standard (yellow-green fluorescent 1- $\mu\text{m}$  beads, Molecular Probes, Invitrogen) was added to the sample prior to analysis. Different virus groups (V1, V2, and V3) could be clearly discriminated on the basis of the green fluorescence and side scatter signature (Fig. 2B). Data were analyzed by the freeware CYTOWIN (<http://sb-roscoff.fr/phyto/cyto.html>). Because of graphic software constraints, some viral particles may appear off-scale on the side scatter signal (Fig. 2B). However, the discriminator was set on the green fluorescence signal; therefore, all particles that may appear off-scale are actually computed in the total number of viruses.

**Virus diversity**—Virus diversity was examined on a 5-liter sample by pulsed-field gel electrophoresis (PFGE) as described by Larsen et al. (2001). Samples were concen-

trated by 30 kDa of MWCO (molecular weight cut-off) ultrafiltration (Vivaflow 200, Vivascience) and clarified of bacteria and cell debris by low-speed centrifugation ( $10,000 \times g$ , 30 min at  $4^\circ\text{C}$ , fixed-angle rotor F-34-6-38, Eppendorf 5810R). Supernatant was harvested by ultracentrifugation ( $141,000 \times g$ , 2 h at  $8^\circ\text{C}$ , fixed-angle rotor TFT 55.38 rotor, Centrikon T-1080, Kontron Instruments), and pellets were resuspended in SM buffer. Three plugs of this concentrate were prepared in molten 1.5% (w/v) InCert agarose (Cambrex Bioscience) and digested overnight at  $30^\circ\text{C}$  in a lysis buffer ( $250 \text{ mmol L}^{-1}$  EDTA, 1% sodium dodecyl sulfate [v/v], 1 mg  $\text{mL}^{-1}$  proteinase K, Sigma-Aldrich). Samples were loaded onto a 1% SeaKem GTG agarose gel (Cambrex Bioscience) in  $1 \times$  Tris-borate-EDTA (TBE) buffer. The gel was run with a Bio-Rad DR-II CHEF Cell unit operating at  $6 \text{ V cm}^{-1}$  at  $14^\circ\text{C}$  in  $0.5 \times$  TBE tank buffer. Two different pulse ramp settings were used for an optimal sizing of viral genomes. Besides a pulse ramp of 1–6 s for 20 h to examine the smaller virus genomes, a pulse ramp of 8–30 s for 20 h was used to discriminate the larger virus genomes. After electrophoresis, gels were stained for 1 h with SYBR Green I ( $1 \times 10^{-4}$  of commercial solution, Molecular Probes, Invitrogen) and destained for 10 min in MilliQ (Gradient A10, Millipore) before a digital analysis for fluorescence with a FluorS imager (Bio-Rad). Sizing of the viral genomes was performed against a 5-kb lambda ladder or a lambda concatamers ladder (both Bio-Rad). The relative abundance of the different viral genome sizes was estimated by normalizing the intensity of each detected band by the determined genome size.

## Results

**Picophytoplankton**—Total picophytoplankton abundance varied between 1.2 and  $4.7 \times 10^4$  cells  $\text{mL}^{-1}$  (Fig. 3A). For all stations, the prokaryotic cyanobacteria (*Prochlorococcus* and *Synechococcus*) numerically dominated the picophytoplankton community with an abundance ranging from 1.1 to  $3.8 \times 10^4$  cells  $\text{mL}^{-1}$  (76–95% of the total numerical abundance, Fig. 3A). *Prochlorococcus* was the main contributor, making up for 71–99% of the cyanobacterial abundance. The highest contribution of picoeukaryotes (18% and 24%, Fig. 3A) was found for the southeastern stations of the studied area (Sta. 20 and 33). The smaller-sized picoeukaryote group I generally dominated over group II, with abundance between 0.4 and  $5.4 \times 10^3$   $\text{mL}^{-1}$  (up to threefold that of picoeukaryote group II).

In terms of carbon biomass, the picophytoplankton ranged from 1.5 to  $6.0 \mu\text{g C L}^{-1}$ , with the highest values found at Sta. 20 (Fig. 3B). The cyanobacteria *Synechococcus* and *Prochlorococcus* accounted, on average, for  $28\% \pm 14\%$  (range, 3–44%) and  $32\% \pm 17\%$  (range, 20–65%) of the total picophytoplankton carbon biomass, respectively (Fig. 3B). The picoeukaryotes accounted, on average, for  $41\% \pm 9\%$  (range, 30–53%) of the total carbon biomass (Fig. 3B).

**Dilution assay**—The viral lysis dilution assay could be applied successfully to the oligotrophic study site (Figs. 4,

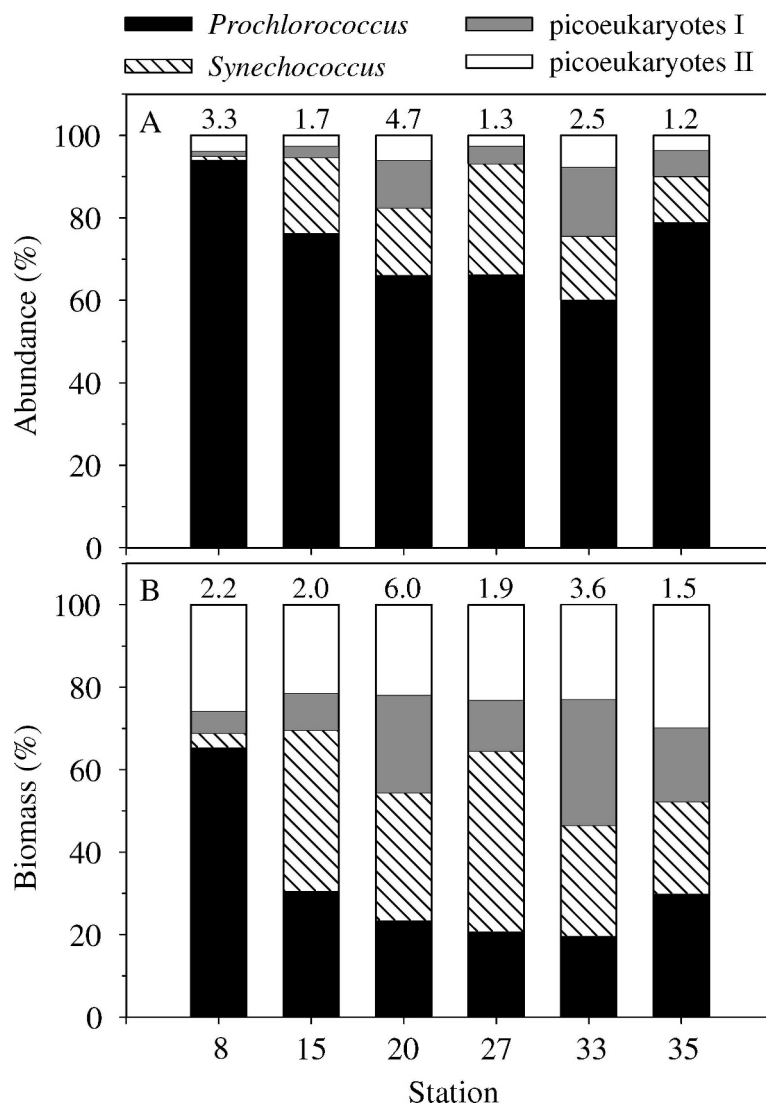


Fig. 3. Contribution of the different picophytoplankton groups to (A) the total picophytoplankton abundance and (B) the total carbon biomass of picophytoplankton. Numbers above the bars indicate (A) the total picophytoplankton abundance ( $\times 10^4 \text{ mL}^{-1}$ ) and (B) the total picophytoplankton carbon biomass ( $\mu\text{g C L}^{-1}$ ).

5; Table 2). Figure 4 depicts the four representative combinations of viral lysis and microzooplankton grazing obtained during the cruise: substantial viral lysis rates with varying microzooplankton grazing (Fig. 4A,B) and vice versa (Fig. 4C,D). As a result, viral-induced mortality greatly varied, depending on the picophytoplankton group examined (Fig. 5; Table 2). The highest viral lysis rates were observed for picoeukaryote group I, with rates ranging from 0.1 to  $0.8 \text{ d}^{-1}$ . Viral lysis rates of the other three groups (picoeukaryote group II, *Synechococcus*, and *Prochlorococcus*) were smaller than  $0.1 \text{ d}^{-1}$ . The microzooplankton grazing on picoeukaryote group I ranged from 0 to  $0.2 \text{ d}^{-1}$ , and on picoeukaryote group II, they varied from 0.1 to  $0.4 \text{ d}^{-1}$ . Comparable grazing rates ( $0.1\text{--}0.3 \text{ d}^{-1}$ ) were obtained for *Synechococcus*, but grazing by microzooplankton on *Prochlorococcus* was generally lower (maximum,  $0.1 \text{ d}^{-1}$ ).

The growth rates for both picoeukaryote groups averaged  $0.4 \text{ d}^{-1}$  (Table 2), with more variation for group I ( $0.2\text{--}0.9 \text{ d}^{-1}$ ) than for group II ( $0.3\text{--}0.6 \text{ d}^{-1}$ ). The growth rate averaged  $0.2 \text{ d}^{-1}$  for both *Synechococcus* ( $0.03\text{--}0.3 \text{ d}^{-1}$ ) and *Prochlorococcus* ( $0.1\text{--}0.2 \text{ d}^{-1}$ ), with the exception of *Prochlorococcus* at Sta. 35 ( $1.3 \text{ d}^{-1}$ ). Occasionally, the viral dilution assay provided unsuccessful results for one or more of the specific algal groups (Sta. 8 and 35), which seem related to very low abundance and/or apparent growth rates in the undiluted samples (the lowest encountered during this study).

*Virus abundance and diversity*—The total virus abundance was comparable for all stations ( $1.6$  to  $1.8 \times 10^7 \text{ virus mL}^{-1}$ ), except for Sta. 35, which showed a higher abundance ( $2.5 \times 10^7 \text{ mL}^{-1}$ ). Within the virus community, group V1 (characterized by the lower nucleic acid green

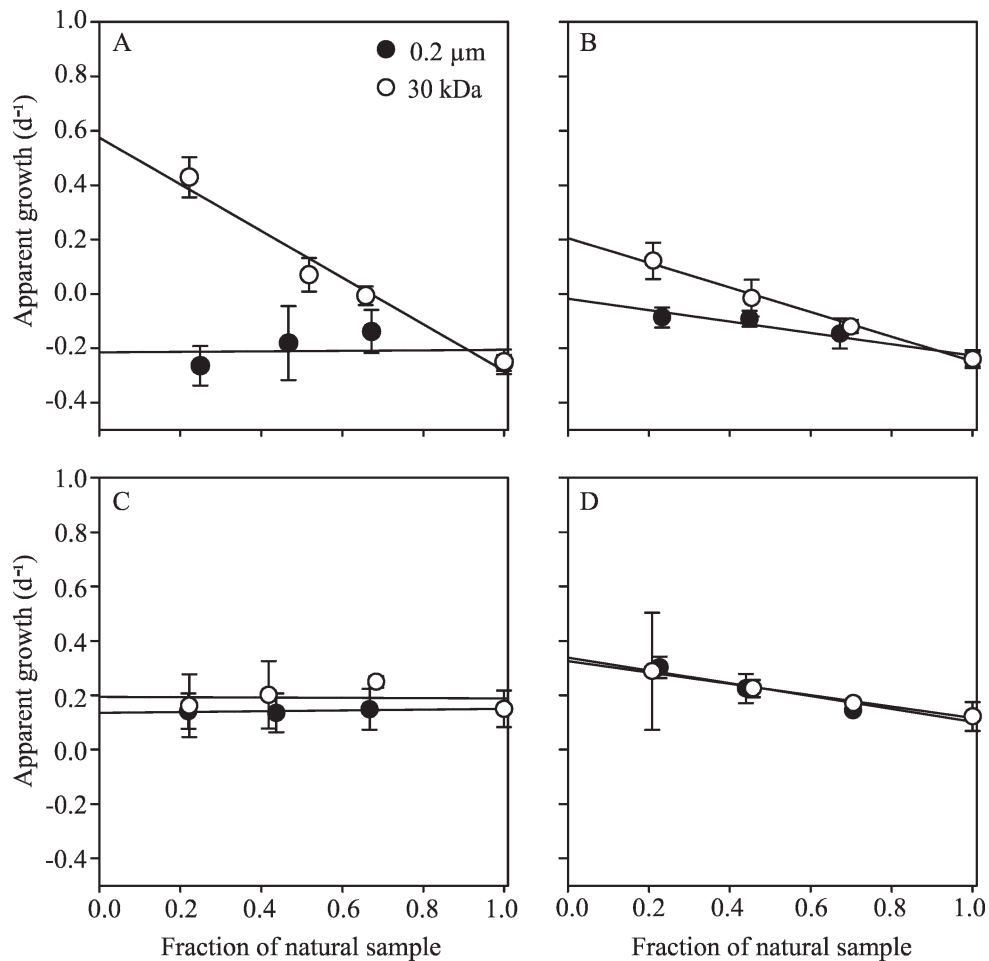


Fig. 4. Representative plots of the viral lysis dilution assay obtained during the cruise for different grazing and viral lysis conditions. (A) Viral lysis but no microzooplankton grazing observed as recorded for picoeukaryote group I at Sta. 35; (B) viral lysis as well as microzooplankton grazing as recorded for picoeukaryote group I at Sta. 33; (C) no viral lysis, no microzooplankton grazing observed as recorded for *Prochlorococcus* at Sta. 15; (D) microzooplankton grazing but no viral lysis observed as recorded for *Synechococcus* at Sta. 33. Parallel dilution experiments were performed in 30-kDa ultrafiltrate (no grazer, no virus) and 0.2- $\mu\text{m}$  (no grazer) filtered seawater. Microzooplankton grazing rates correspond to the regression slope obtained with the 0.2- $\mu\text{m}$  dilution series. Viral lysis rates correspond to the difference of regression coefficients of the 0.2- $\mu\text{m}$  and 30-kDa series. For the readability of the figures, we averaged the triplicate apparent growth for each dilution level. This operation did not affect the estimated mortality rates. The error bars reflect the standard deviation between measurements.

fluorescence, Fig. 2B) dominated and made up 64–73% of the total abundance. The abundance of group V3 (with the highest nucleic acid green fluorescence) represented 5–11% of the total virus community. The highest abundance of this group V3 was recorded at Sta. 8 and 35 ( $2 \times 10^6 \text{ mL}^{-1}$ ), whereas the lowest abundance was found at Sta. 20 ( $0.8 \times 10^6 \text{ mL}^{-1}$ ).

The virus diversity analysis by PFGE displayed four to seven genome sizes per sample, ranging from 35 to 225 kb (Fig. 6). Northern Sta. 8 and 35 showed intense bands for the larger virus genomes (185, 210, and 225 kb) representing, on average, 10% of the total virus community. Sta. 15, 20, 27, and 33 showed only a single 185-kb band of moderate intensity, contributing to 6% of the total virus community. The 65-kb band was the thickest of the smaller viral genomes

(35, 45, 65, 85, 90, and 100 kb), corresponding to an average 38% (28–62%) of the total virus community.

**Daily carbon flow**—The daily carbon produced by the total picophytoplankton community varied largely between stations (Table 3). Despite their low abundance, the picoeukaryotes (groups I and II) contributed for 61% of the total carbon produced (omitting Sta. 8 and 35 because of incomplete data sets). The total picophytoplanktonic carbon losses balanced the total carbon produced, for the most part, comprising, on average, 74% ( $\pm 11$ ). The carbon losses due to viral-induced mortality ranged from 0.1 to 0.3  $\mu\text{g C L}^{-1} \text{ d}^{-1}$ , which almost exclusively originated from the picoeukaryotes ( $97\% \pm 4\%$ ). The total losses due to viral lysis made up 21% of the total picophytoplankton carbon biomass produced per

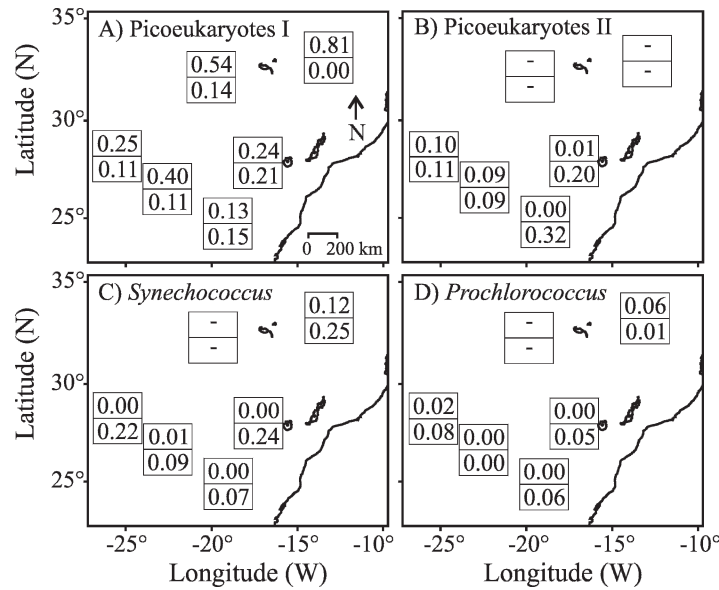


Fig. 5. Overview of viral lysis and microzooplankton grazing rates per station for (A) picoeukaryote group I, (B) picoeukaryote group II, (C) *Synechococcus*, and (D) *Prochlorococcus*. Viral lysis ( $d^{-1}$ ) is shown as the top number, and grazing ( $d^{-1}$ ) is the bottom number.

day (again excluding Sta. 8 and 35). Microzooplankton consumed  $0.1\text{--}0.9 \mu\text{g C L}^{-1} \text{d}^{-1}$ , which originated equally from the picocyanobacteria and the picoeukaryotes. The highest grazing-mediated carbon losses were observed for Sta. 20 and 33 ( $0.9$  and  $0.7 \mu\text{g C L}^{-1} \text{d}^{-1}$ , respectively).

### Discussion

The traditional dilution assay originally developed to estimate microzooplankton grazing on phytoplankton (Landry and Hassett 1982) is routinely used in a wide range of marine systems, including open-ocean oligotrophic

habitats (Calbet and Landry 2004). This is, however, the first published report of a viral lysis dilution assay applied to an oligotrophic environment. The present study shows that viral lysis can be an important loss factor for the picophytoplankton ( $<3 \mu\text{m}$  in diameter) in the oligotrophic waters in the subtropical northeastern Atlantic Ocean. In particular, picoeukaryote group I ( $<1.5 \mu\text{m}$  in diameter) was prone to high viral-mediated mortality (with rates of up to  $0.8 \text{d}^{-1}$ ).

*Methodological aspects*—It is important to note that this method detects only the lysis of algal hosts that are newly

Table 2. Viral lysis, microzooplankton grazing, and growth rates calculated from the dilution assay for the four phytoplankton groups. Asterisks correspond to the significance ( $t$ -test) of the mortality and growth rates.

	Station					
	8	15	20	27	33	35
Viral lysis rates ( $d^{-1}$ )						
Picoeukaryotes I	0.54*	0.40*	0.13***	0.25**	0.24*	0.81*
Picoeukaryotes II	—†	0.09***	0.00***	0.10***	0.01***	—
<i>Synechococcus</i>	—	0.01***	0.00***	0.00***	0.00***	0.12*
<i>Prochlorococcus</i>	—	0.00***	0.00***	0.02***	0.00***	0.06***
Grazing rates ( $d^{-1}$ )						
Picoeukaryotes I	0.14*	0.11*	0.15**	0.11***	0.21*	0.00***
Picoeukaryotes II	—	0.09***	0.36*	0.11***	0.20*	—
<i>Synechococcus</i>	—	0.09***	0.07**	0.22*	0.24*	0.25*
<i>Prochlorococcus</i>	—	0.00***	0.06***	0.08***	0.05*	0.01***
Growth rates ( $d^{-1}$ )						
Picoeukaryotes I	0.88*	0.44*	0.26*	0.31*	0.20*	0.54*
Picoeukaryotes II	—	0.30*	0.51*	0.39*	0.61*	—
<i>Synechococcus</i>	—	0.07**	0.06*	0.18*	0.31*	0.28*
<i>Prochlorococcus</i>	—	0.19*	0.20*	0.12*	0.30*	1.30*

† —, unsuccessful.

\*  $p < 0.05$ ; \*\*  $p = 0.05\text{--}0.1$ ; \*\*\*  $p > 0.1$ .

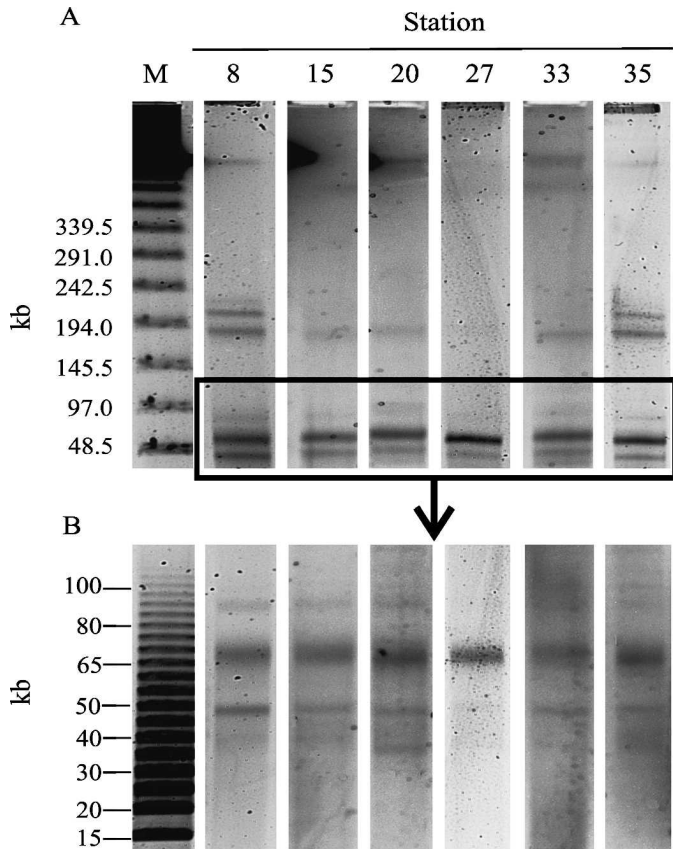


Fig. 6. Virus PFGE fingerprint for each station studied. (A) The upper electrophoretic profiles represent large virus genomes (50–300 kb, including putative algal viruses). Their genome size was determined with the phage lambda concatamers ladder (M, panel A). (B) The bottom profiles show smaller virus genomes (10–100 kb), which were compared to a 5-kb lambda ladder (M, panel B). Some of the bands may not be visible here but could be seen on the original picture. Each gel lane was aligned with the ladder and shown precisely as it fell in the gel it was actually run in (and relative to the standard in that gel).

infected during the incubation period (*see* Baudoux et al. 2006 for a more detailed discussion). An important assumption of the dilution assay is that phytoplankton losses are proportional to the dilution effect on the abundance of the mortality agents. This implies that a single round of infection should be detected and, thus, that the host's cell lysis must occur later than 12 h after infection but within the 24-h incubation. Most studies of algal host–virus model systems (including prokaryotic algal hosts) show that the time to cell lysis upon viral infection is indeed within 24 h (Mann 2003; Brussaard 2004a). It is, furthermore, assumed that there is no preferential grazing by microzooplankton. For substantial preferential grazing on infected cells, viral lysis would be underestimated, as suggested earlier (Ruardij et al. 2005). Another aspect of concern is that there is no substantial loss of virus during the incubation. Grazing by heterotrophic nanoflagellates (HNFs) could potentially be a source of viral loss, but reported rates of viral removal by HNFs are rather low ( $\leq 0.3\% \text{ d}^{-1}$ , Gonzalez and Suttle 1993).

In spite of these considerations, this method has the benefit of excluding the use of a conversion factor and of minimizing the handling of the sample. Its utilization has been validated across different algal host taxa (Evans et al. 2003; Baudoux et al. 2006). The consistency of the viral lysis rates obtained by this methodology with other means for assessing cell lysis furthermore provides confidence in the suitability of this method to infer the effect of viruses on phytoplankton mortality (Baudoux et al. 2006). Interestingly, we found a strong positive linear relationship ( $r = 0.82$ ,  $n = 6$ ,  $p = 0.01$ ) between the viral lysis rates of picoeukaryote group I and the abundance of virus presenting an enhanced stained DNA fluorescence signal (group V3) that most likely comprises algal viruses (Brussaard 2004b).

*Picoeukaryotes*—Viruses were substantial mortality agents for the picoeukaryotic community, responsible, on average, for 71% and 26% of the mortality of picoeukaryote groups I and II, respectively. Acknowledging that our data set includes only six sampling stations, we did record clear differences in the viral-induced mortality rates of the picoeukaryotes and in the relative effect of viruses across the system. The highest viral lysis rates were recorded for picoeukaryote group I at the northern Sta. 8 and 35 ( $0.5$  and  $0.8 \text{ d}^{-1}$ ) and the southwestern Sta. 15 ( $0.4 \text{ d}^{-1}$ ). At these stations, viral lysis was responsible for 80–100% of the total picoeukaryote cell losses. Sta. 8, 15, and 35 also had the highest contribution of viruses with larger-sized genomes (185, 210, and 225 kb), a characteristic feature of the virus family *Phycodnaviridae* that infects eukaryotic algae (*ICTVdB—The Universal Virus Database*, version 4. <http://www.ncbi.nlm.nih.gov/ICTVdb/ICTVdB/>).

The growth rate of picoeukaryote group I at these stations with increased viral lysis rates was higher ( $0.5$ – $0.9 \text{ d}^{-1}$ ) than at the other stations. Earlier studies conducted under controlled conditions showed that the algal host's growth rate can influence the interactions between virus and host and, hence, viral lysis rate (Bratbak et al. 1998). In these studies, optimal growth conditions of the algal host resulted in enhanced virus production. Thereby, we speculate that the relatively high growth rates of picoeukaryote group I at Sta. 8, 15, and 35 enhanced the impact of viruses as mortality agents ( $0.5$ – $0.8 \text{ d}^{-1}$ ).

The contribution of microzooplankton grazing as a loss factor was highest at southeastern Sta. 20 and 33. At these stations, grazing made up 50% of the total mortality for picoeukaryote group I (0–30% at the other stations) and 95–100% for picoeukaryote group II (50% at the other stations). Although it is difficult to conclude on the factors underlying the difference in mortality processes (viral lysis vs. microzooplankton grazing), it is noteworthy that picoeukaryote abundance was 4- to 10-fold higher at these stations (Sta. 20 and 33) than at the other stations. These differences could be due to different water types that may originate from the proximity of coastal areas and/or the Canary Current that flows along the African coast and entrains upwelling waters. The higher abundance in picoeukaryotes at these southeastern stations may exceed the threshold level of prey for microzooplankton, resulting

Table 3. Daily carbon production and daily carbon losses mediated by viral lysis and microzooplankton grazing for the respective picophytoplankton groups.

	Station					
	8	15	20	27	33	35
C production ( $\mu\text{g C L}^{-1} \text{d}^{-1}$ )						
Picoeukaryotes I	0.11	0.08	0.37	0.07	0.19	0.13
Picoeukaryotes II	—	0.14	0.72	0.18	0.61	—
<i>Synechococcus</i>	—	0.05	0.11	0.14	0.31	0.09
<i>Prochlorococcus</i>	—	0.13	0.30	0.05	0.24	1.14
Total	$\geq 0.11$	0.40	1.50	0.44	1.35	$\geq 1.36$
Total C losses ( $\mu\text{g C L}^{-1} \text{d}^{-1}$ )						
Picoeukaryotes I	0.09	0.09	0.40	0.08	0.43	0.19
Picoeukaryotes II	—	0.08	0.51	0.10	0.21	—
<i>Synechococcus</i>	—	0.08	0.13	0.18	0.24	0.12
<i>Prochlorococcus</i>	—	0.00	0.09	0.04	0.04	0.06
Total	$\geq 0.09$	0.25	1.13	0.40	0.92	$\geq 0.37$
Viral lysis C losses ( $\mu\text{g C L}^{-1} \text{d}^{-1}$ )						
Picoeukaryotes I	0.07	0.07	0.18	0.06	0.23	0.19
Picoeukaryotes II	—	0.04	0.00	0.05	0.01	—
<i>Synechococcus</i>	—	0.01	0.00	0.00	0.00	0.04
<i>Prochlorococcus</i>	—	0.00	0.00	0.01	0.00	0.05
Total	$\geq 0.07$	0.12	0.18	0.11	0.24	$\geq 0.28$
Grazing C losses ( $\mu\text{g C L}^{-1} \text{d}^{-1}$ )						
Picoeukaryotes I	0.02	0.02	0.21	0.02	0.20	0.00
Picoeukaryotes II	—	0.04	0.50	0.05	0.20	—
<i>Synechococcus</i>	—	0.07	0.13	0.18	0.24	0.08
<i>Prochlorococcus</i>	—	0.00	0.09	0.03	0.05	0.01
Total	$\geq 0.02$	0.13	0.94	0.28	0.68	$\geq 0.09$

in enhanced grazing rates. Selective grazing can also contribute to the different phytoplankton community.

*Prokaryotes*—Despite their numerical dominance, *Synechococcus* and *Prochlorococcus* showed low viral-induced mortality rates. Viral lysis rates averaged  $0.02 \pm 0.05 \text{ d}^{-1}$  for *Synechococcus* and  $0.02 \pm 0.03 \text{ d}^{-1}$  for *Prochlorococcus*, corresponding to a removal of 1% and 3% of the standing stock per day. These estimates are comparable to previous results indicating that ca.  $3\% \text{ d}^{-1}$  of the *Synechococcus* population undergoes viral lysis, as determined by indirect viral lysis assays (as cited in Garza and Suttle 1998). In offshore oligotrophic waters, cyanobacteria are found in relatively high numbers, but infectious *Synechococcus* and *Prochlorococcus* phages occur in low abundance (Sullivan et al. 2003). Sullivan et al. (2003) even argued that these “low [cyanophages] titers in areas of high host abundance seem to be characteristic features of the open ocean.” Such a situation will result in reduced contact rates between the potential host and co-occurring virus and may have been a reason for the low reported viral lysis rates for the prokaryotes. In agreement with the low viral lysis rates, the percentage of dead prokaryotic phytoplankton, as determined with the SYTOX Green dye, was low (Veldhuis unpubl. data). Agusti (2004) also observed a good viability of the autotrophic prokaryotes in the same geographical area.

The generally high genotypic diversity within the populations of *Synechococcus* and *Prochlorococcus* (Scan-

lan and West 2002) as well as the ability of cyanobacteria to acquire cyanophage resistance (Waterbury and Valois 1993) may have been other factors reducing the effect of cyanophages as mortality agents. As hypothesized earlier for the picoeukaryotes, low viral-induced mortality may also be related to the moderately low growth rates recorded for *Synechococcus* ( $0.2 \pm 0.1 \text{ d}^{-1}$ ) and *Prochlorococcus* ( $0.2 \pm 0.05 \text{ d}^{-1}$ , with the exception of Sta. 35, where growth reached  $1.3 \text{ d}^{-1}$ ) during our study. *Synechococcus* typically distributes in the surface oceanic layers, and lower growth rates at DCM depths are usually reported (Partensky et al. 1996; Liu et al. 1998). Conversely, *Prochlorococcus* cells do extend into deeper waters, where they generally grow faster than *Synechococcus* (ca.  $0.69 \text{ d}^{-1}$ ; Partensky et al. 1999). Growth rates as low as  $0.1 \text{ d}^{-1}$  have, however, been observed at similar depths in the northern subtropical Pacific Ocean (Liu et al. 1995), which substantiates the moderately low values here reported.

*Synechococcus* was mainly controlled by microzooplankton grazing, and the recorded rates ( $0.1\text{--}0.25 \text{ d}^{-1}$ ) were consistent with those obtained in the same geographical area at similar depths (on average,  $0.3 \text{ d}^{-1}$ ; Quevedo and Anadón 2001). Grazing on *Prochlorococcus* was substantially lower (on average,  $0.04 \pm 0.03 \text{ d}^{-1}$ ) than observed for *Synechococcus*, indicating that both prokaryotic groups underwent different loss mechanisms. The occurrence of differential grazing losses has already been reported for *Synechococcus* and *Prochlorococcus* under controlled conditions. For example, some ciliates showed a marked preference for

*Synechococcus* against *Prochlorococcus* (Christaki et al. 1999). Similar observations were reported for some HNFs, but preferential grazing against *Prochlorococcus* occurred only when both preys coexisted at similar concentrations (Guillou et al. 2001). In the case of HNF grazing on the autotrophic picocyanobacteria, we cannot exclude that a trophic cascade was induced that may have resulted in reduced grazing rates. The overall low total loss rates, in combination with the moderately low growth rates, may partially explain the numerical dominance of *Prochlorococcus* (60–94% of total abundance) at the studied stations.

*Implications for geochemical fluxes*—The total CP by the picophytoplankton at the DCM in the northeastern subtropical Atlantic Ocean (October 2002) was largely balanced by the losses due to grazing and viral lysis. This illustrates a situation close to steady state, as can be expected for oligotrophic ecosystems. The carbon losses mediated by viral lysis accounted, on average, for 21% of the total CP by the picophytoplankton community. This percentage is higher than the 2–10% loss assumed by Wilhelm and Suttle (1999), applying the revised steady-state model of Jumars et al. (1989). These lower values may be caused by the limited number of studies that were incorporated into the model or by the restricted number of potential algal hosts taken into account. But Wilhelm and Suttle (1999) also grouped all phytoplankton without making a distinction between eukaryotes and prokaryotes. Our results clearly show that the influence of viral lysis on carbon cycling varied, depending on the picophytoplankton group. Picoeukaryotes were responsible for 97% of the cellular carbon released by viral lysis. Hence, it appears essential to investigate viral lysis for all co-occurring phytoplankton groups to obtain a better insight into the influence of algal viruses on carbon cycling.

Next to the considerable release of carbon through picoeukaryote viral lysis, a parallel study conducted during IRONAGES III suggested that the lysis of picoeukaryote group I was an important source of iron-organic ligand at DCM (Gerringa et al. 2006). Iron availability is considered an important colimiting factor for marine ecosystem productivity, and most of the total dissolved iron in seawater is complexed by dissolved organic ligands and constitutes, as such, the largest potential pool of bioavailable iron to marine plankton (Rue and Bruland 1995). Because viral-induced mortality was the main source of cell loss for picoeukaryote group I (this study), viral lysis seems to play a critical role in the recycling of organically complexed iron in the oligotrophic northeastern subtropical Atlantic Ocean. Other authors have drawn similar conclusions from laboratory and experimental studies (Poorvin et al. 2004).

In contrast to the picoeukaryotes, the prokaryotes did not substantially contribute to the release of carbon through viral lysis. Instead, microzooplankton grazing accounted for most of the prokaryote carbon losses (97%). Overall, microzooplankton consumed 52% ± 14% of the total picophytoplanktonic CP. This value is only slightly lower than the averaged estimate of 67% of phytoplankton production consumed by microzooplank-

ton, which was based on a large data set (Calbet and Landry 2004). Our sampling at the DCM might be responsible for this difference (the sampling depth considered in Calbet and Landry [2004] is not clear).

In summary, the adapted dilution assay that estimates both viral lysis and microzooplankton grazing was successfully applied to the oligotrophic waters of the northeastern subtropical Atlantic Ocean. The effect of viruses on picophytoplankton mortality was algal group-specific and particularly high for the picoeukaryotes. Given that this study represents the first quantification of viral mortality rates on picophytoplankton, the prevalence of such rates for discrete populations should be explored in other marine sites to verify their broader applicability.

## References

- AGUSTI, S. 2004. Viability and niche segregation of *Prochlorococcus* and *Synechococcus* cells across the Central Atlantic Ocean. *Aquat. Microb. Ecol.* **36**: 53–59.
- , M. P. SATTÀ, M. P. MURA, AND E. BENAVENT. 1998. Dissolved esterase activity as a tracer of phytoplankton lysis: Evidence of high phytoplankton lysis rates in the northwestern Mediterranean. *Limnol. Oceanogr.* **43**: 1836–1849.
- BAUDOUX, A.-C., A. A. M. NOORDELOOS, M. J. W. VELDHUIS, AND C. P. D. BRUSSAARD. 2006. Virally induced mortality of *Phaeocystis globosa* during two spring blooms in temperate coastal waters. *Aquat. Microb. Ecol.* **44**: 207–217.
- BERTLISSON, S., O. BERGLUND, D. M. KARL, AND S. W. CHISHOLM. 2003. Elemental composition of marine *Prochlorococcus* and *Synechococcus*: Implications for the ecological stoichiometry of the sea. *Limnol. Oceanogr.* **48**: 1721–1731.
- BRATBAK, G., A. JACOBSEN, M. HELDAL, K. NAGASAKI, AND F. THINGSTAD. 1998. Virus production in *Phaeocystis pouchetii* and its relation to host cell growth and nutrition. *Aquat. Microb. Ecol.* **16**: 1–9.
- BRUSSAARD, C. P. D. 2004a. Viral control of phytoplankton populations—a review. *J. Eukaryot. Microbiol.* **51**: 125–138.
- . 2004b. Optimization of procedures for counting viruses by flow cytometry. *Appl. Environ. Microbiol.* **70**: 1506–1513.
- CALBET, A., AND M. R. LANDRY. 2004. Phytoplankton growth, microzooplankton grazing, and carbon cycling in marine systems. *Limnol. Oceanogr.* **49**: 51–57.
- CHRISTAKI, U., S. JACQUET, J. R. DOLAN, D. VAULOT, AND F. RASSOULZADEGAN. 1999. Growth and grazing on *Prochlorococcus* and *Synechococcus* by two marine ciliates. *Limnol. Oceanogr.* **44**: 52–61.
- DURAND, M. D., R. E. GREEN, H. M. SOSIK, AND R. J. OLSON. 2002. Diel variations in optical properties of *Micromonas pusilla* (Prasinophyceae). *J. Phycol.* **38**: 1132–1142.
- EVANS, C., S. D. ARCHER, S. JACQUET, AND W. H. WILSON. 2003. Direct estimates of the contribution of viral lysis and microzooplankton grazing to the decline of a *Micromonas* spp. population. *Aquat. Microb. Ecol.* **30**: 207–219.
- GARZA, D. R., AND C. A. SUTTLE. 1998. The effect of cyanophages on the mortality of *Synechococcus* spp. and selection for UV resistant viral communities. *Microb. Ecol.* **36**: 281–292.
- GERRINGA, L. J. A., M. J. W. VELDHUIS, K. R. TIMMERMANS, G. SARTHOU, AND H. J. W. DE BAAR. 2006. Co-variance of dissolved Fe-binding ligands with phytoplankton characteristics in the Canary Basin. *Mar. Chem.* **102**: 276–290.
- GONZALEZ, J. M., AND C. A. SUTTLE. 1993. Grazing by marine nanoflagellate on viruses and virus-sized particles: Ingestion and digestion. *Mar. Ecol. Prog. Ser.* **94**: 1–10.

- GUILLOU, L., S. JACQUET, M.-J. CHRÉTIENNOT-DINET, AND D. VAULOT. 2001. Grazing impact of two small heterotrophic flagellates on *Prochlorococcus* and *Synechococcus*. *Aquat. Microb. Ecol.* **26**: 201–207.
- JUMARS, P. A., D. L. PENRY, J. A. BAROSS, M. J. PERRY, AND B. W. FROST. 1989. Closing the microbial loop—dissolved carbon pathway to heterotrophic bacteria from incomplete ingestion, digestion and absorption in animals. *Deep-Sea Res.* **36**: 483–495.
- LANDRY, M. R., J. CONSTANTINOU, M. LATASA, S. L. BROWN, R. R. BIDIGARE, AND M. E. ONDRUSEK. 2000. Biological response to iron fertilization in the eastern equatorial Pacific (IronEx II). Dynamics of phytoplankton growth and microzooplankton grazing. *Mar. Ecol. Prog. Ser.* **201**: 57–72.
- , AND R. P. HASSETT. 1982. Estimating the grazing impact of marine micro-zooplankton. *Mar. Biol.* **67**: 283–288.
- LARSEN, A., AND OTHERS. 2001. Population dynamics and diversity of phytoplankton, bacteria and viruses in a seawater enclosure. *Mar. Ecol. Prog. Ser.* **221**: 47–57.
- LI, W. K. W. 1994. Primary production of prochlorophytes, cyanobacteria, and eukaryotic ultraphytoplankton—measurements from flow cytometric sorting. *Limnol. Oceanogr.* **39**: 169–175.
- LIU, H. B., L. CAMPBELL, AND M. R. LANDRY. 1995. Growth and mortality rates of *Prochlorococcus* and *Synechococcus* measured with a selective inhibitor technique. *Mar. Ecol. Prog. Ser.* **116**: 277–287.
- , ———, ———, H. A. NOLLA, S. L. BROWN, AND J. CONSTANTINOU. 1998. *Prochlorococcus* and *Synechococcus* growth rates and contributions to production in the Arabian Sea during the 1995 Southwest and Northeast monsoons. *Deep-Sea Res.* **45**: 2327–2352.
- MANN, N. H. 2003. Phages of the marine cyanobacterial picophytoplankton. *FEMS Microbiol. Rev.* **27**: 17–34.
- MOON-VAN DER STAAY S. Y., R. DE WACHTER, AND D. VAULOT. 2001. Oceanic 18S rDNA sequences from picoplankton reveal unsuspected eukaryotic diversity. *Nature* **409**: 607–610.
- MÜHLING, M., AND OTHERS. 2005. Genetic diversity of marine *Synechococcus* and co-occurring cyanophage communities: Evidence for viral control of phytoplankton. *Environ. Microbiol.* **7**: 499–508.
- PARTENSKY, F., J. BLANCHOT, F. LANTOINE, J. NEVEUX, AND D. MARIE. 1996. Vertical structure of picophytoplankton at different trophic sites of the tropical northeastern Atlantic Ocean. *Deep-Sea Res.* **43**: 1191–1213.
- , W. R. HESS, AND D. VAULOT. 1999. *Prochlorococcus*, a marine photosynthetic prokaryote of global significance. *Microbiol. Mol. Biol. Rev.* **63**: 106–127.
- POORVIN, L., J. M. RINTA-KANTO, D. A. HUTCHINS, AND S. W. WILHELM. 2004. Viral release of iron and its bioavailability to marine plankton. *Limnol. Oceanogr.* **49**: 1734–1741.
- QUEVEDO, M., AND R. ANADÓN. 2001. Protist control of phytoplankton growth in the subtropical northeast Atlantic. *Mar. Ecol. Prog. Ser.* **221**: 29–38.
- RAVEN, J. A. 1998. The twelfth Tansley Lecture. Small is beautiful: The picophytoplankton. *Funct. Ecol.* **12**: 503–513.
- RUARDIJ, P., M. J. W. VELDHUIS, AND C. P. D. BRUSSAARD. 2005. Modeling the bloom dynamics of the polymorphic phytoplankter *Phaeocystis globosa*: Impact of grazers and viruses. *Harmful Algae* **4**: 941–963.
- RUE, E. L., AND K. W. BRULAND. 1995. Complexation of iron (III) by natural organic-ligands in the Central North Pacific as determined by a new competitive ligand equilibration adsorptive cathodic stripping voltammetric method. *Mar. Chem.* **50**: 117–138.
- SCANLAN, D. J., AND N. J. WEST. 2002. Molecular ecology of the marine cyanobacterial genera *Prochlorococcus* and *Synechococcus*. *FEMS Microbiol. Ecol.* **40**: 1–12.
- SHORT, S. M., AND C. A. SUTTLE. 2003. Temporal dynamics of natural communities of marine algal viruses and eukaryotes. *Aquat. Microb. Ecol.* **32**: 107–119.
- SULLIVAN, M. B., J. B. WATERBURY, AND S. W. CHISHOLM. 2003. Cyanophages infecting the oceanic cyanobacterium *Prochlorococcus*. *Nature* **424**: 1047–1051.
- VELDHUIS, M. J. W., AND G. W. KRAAY. 2004. Phytoplankton in the subtropical Atlantic Ocean: Towards a better assessment of biomass and composition. *Deep-Sea Res.* **51**: 507–530.
- WATERBURY, J. B., AND F. W. VALOIS. 1993. Resistance to co-occurring phages enables marine *Synechococcus* communities to coexist with cyanophages abundant in seawater. *Appl. Environ. Microbiol.* **59**: 3393–3399.
- WILHELM, S. W., AND C. A. SUTTLE. 1999. Viruses and nutrient cycles in the sea. *BioScience* **49**: 781–788.
- WORDEN, A. Z., J. K. NOLAN, AND B. PALENIK. 2004. Assessing the dynamics and ecology of marine picophytoplankton: The importance of the eukaryotic component. *Limnol. Oceanogr.* **49**: 168–179.

Received: 17 August 2006

Accepted: 7 June 2007

Amended: 2 August 2007